Plate and Column Efficiencies of Continuous Rectifying Columns for Binary Mixtures:

K. ONDA, E. SADA, K. TAKAHASHI, and S. A. MUKHTAR

Department of Chemical Engineering
University of Nagoya, Nagoya, Japan

I. Plate Efficiencies

In the design of the distillation column, the plate efficiency plays an important role. The plate efficiency has been defined as Murphree's plate efficiency with the vapor composition in equilibrium with the liquid leaving the plate. This efficiency is reasonable only when the liquid is well mixed (as described in the later sections) and there is no composition gradient of the liquid on the plate. In practice, however, the liquid composition will vary as the liquid flows on the plate. In the case of larger columns and systems of large relative volatilities, Murphree's plate efficiencies have been found to be more than 100%.

In our previous paper (*1*),† it was pointed out that at a fixed point efficiency E_{OG}† Murphree's plate efficiency $(E_{MV})_1$, based on the vapor in equilibrium with the liquid leaving the plate, decreases with the increase of reflux ratio, and plate efficiency $(E_{MV})_0$, based on the vapor composition in equilibrium with the liquid entering the plate, increases with the increase of reflux ratio. A modified plate efficiency was therefore defined as

$$(E_{MV})_{1/2} = \frac{y''_n - y''_{n-1}}{(y_n^*) - y''_{n-1}} \tag{1}$$

where (y_n^*) is the vapor composition in equilibrium with the liquid at the center of the plate.

If the liquid flows unidirectionally on the plate as a plug flow, the relation between the plate efficiencies and the point efficiency is shown in Figure 1. For a fixed point efficiency, Murphree's plate efficiency $(E_{MV})_1$, which is shown with the broken line, increases with λ where $\lambda = mV/L$, and $(E_{MV})_0$ decreases with λ as shown with the dotted line. The modified plate efficiency $(E_{MV})_{1/2}$, however, does not vary so much with the change of λ as shown with the solid line.

Taking into account the mixing of the liquid on a plate, Figure 2 shows the relation between the plate efficiency and the point efficiency. For a fixed Peclet's number N_{Pe}, the variation of $(E_{MV})_{1/2}/E_{OG}$ for λ is much smaller than that of $(E_{MV})_1/E_{OG}$. In the case of $\lambda E_{OG} < 1$ (this condition holds for almost all the practical columns), the value of $(E_{MV})_{1/2}/E_{OG}$ is less than 1.04 for any value of N_{Pe},

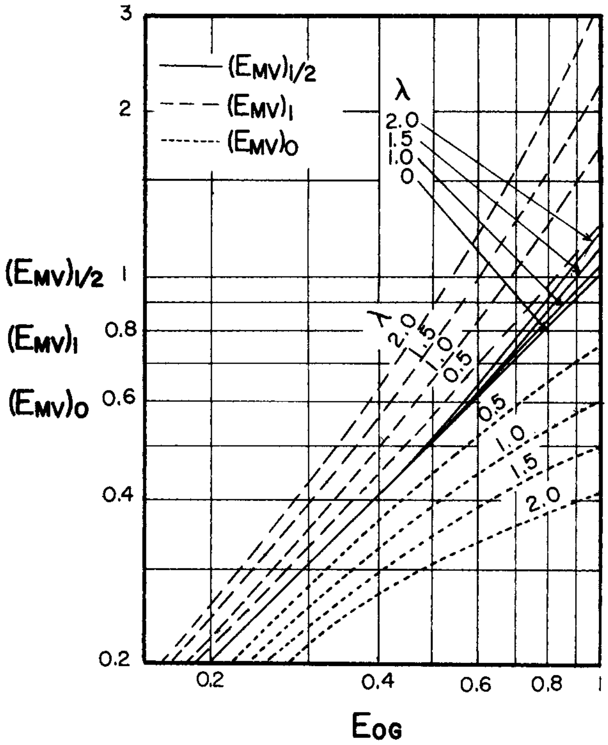

Fig. 1. Relations between plate efficiencies and point efficiency for various values of λ.

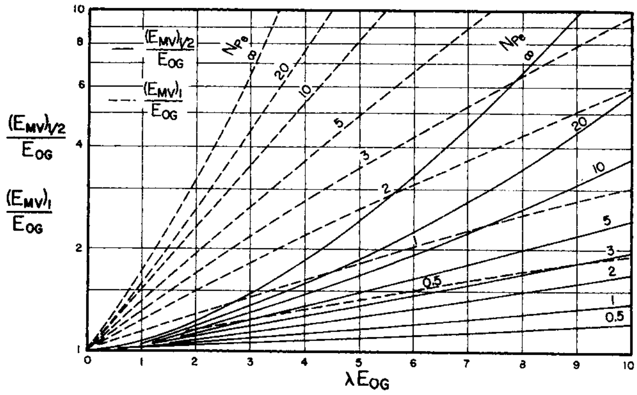

Fig. 2. Variation of $(E_{MV})_{1/2}/E_{OG}$ and $(E_{MV})_1/E_{OG}$ with λE_{OG} for various values of Peclet's number N_{Pe}.

Correspondence concerning this article should be addressed to Prof. K. Onda.

† References and notation are listed at the end of Part II.

and the following relation holds within 4% error

$$(E_{MV})_{1/2} = E_{OG} \qquad (2)$$

In accordance with the modified plate efficiency $(E_{MV})_{1/2}$, the method of calculating the number of theoretical plates is developed, and the minimum number of theoretical plates is discussed.

In the actual columns, the composition of the liquid at the center of the plate is not usually measured; therefore, the mean of compositions of the liquid at the inlet and the outlet of the plate has been taken as a standard, and the efficiencies calculated with this composition are designated as $(E_{MV})'_{1/2}$. The modified plate efficiencies $(E_{MV})'_{1/2}$ are calculated with the reported data of the distillation experiments (2), (3), and (5), and the reflux ratio is shown to have little effect on the plate efficiency $(E_{MV})'_{1/2}$. The modified plate efficiency $(E_{MV})'_{1/2}$ is correlated with the several dimensionless groups comprising most of the variables affecting efficiency, and empirical equations are presented.

CALCULATION OF NUMBER OF THEORETICAL PLATES

Graphical Method

To determine the number of the theoretical plates for the distillation column, McCabe and Thiele's method (6) is most commonly used. This method involves stepwise construction between the operating lines and the equilibrium curve, assuming no composition gradient of the liquid on the plate, and takes into account the vapor in equilibrium with the liquid leaving the plate. In practice, however, the liquid composition varies from inlet to outlet of the plate. It seems that the larger the column diameter, the greater the composition difference on the plate.

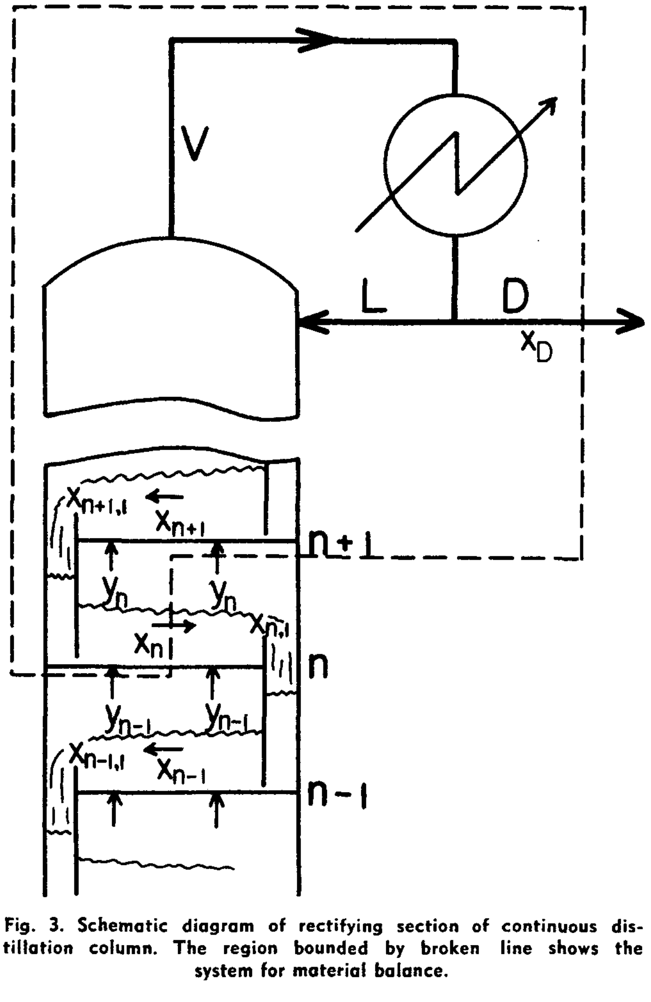

Fig. 3. Schematic diagram of rectifying section of continuous distillation column. The region bounded by broken line shows the system for material balance.

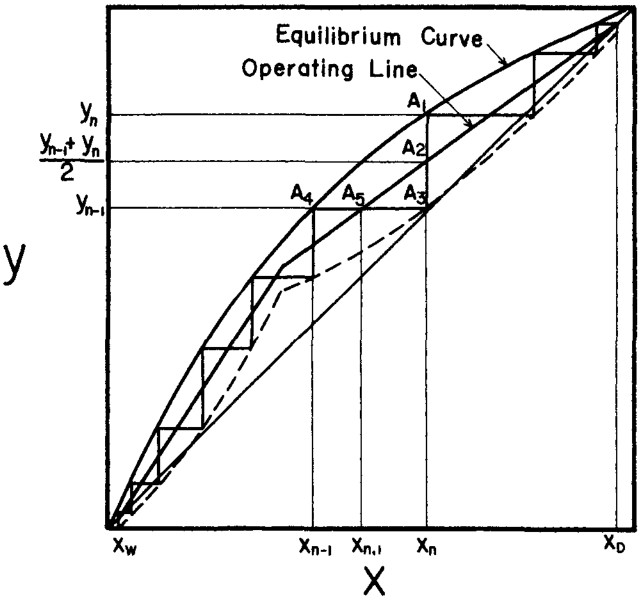

Fig. 4. Stepwise construction for plug flow of liquid on the plate.

Taking into account the liquid composition gradient, the method of stepwise construction for the unidirectional plug flow of the liquid is given with the assumption that the liquid and the vapor flow rates are constant over the sections of the column between feeds and sidedraws. The material balance of the specified component for the system enclosed by broken line in Figure 3 is

$$\frac{V}{2}(y_{n-1} + y_n) = Lx_n + Dx_D \qquad (3)$$

where x_n is the liquid composition at the center of n^{th} plate, and the plate numbers are counted upward from the bottom to the top.

Equation (3) is divided by V as

$$\frac{y_{n-1} + y_n}{2} = \left(\frac{L}{V}\right) x_n + \left(\frac{D}{V}\right) x_D \qquad (4)$$

Equation (4) represents the operating line for the enriching section. The operating line for the exhausting section can be obtained similarly

$$\frac{y_{(n-1)0} + y_{n0}}{2} = \left(\frac{L'}{V'}\right) x_{n0} - \left(\frac{W}{V'}\right) x_W \qquad (5)$$

Also, for an ideal plate, the vapor is assumed to be in equilibrium with the liquid at the center of the plate

$$y_n \text{ equilibrium with } x_n \qquad (6)$$

For binary components system, Equations (4) and (6) are expressed on x-y diagram as shown in Figure 4. Then, the graphical procedure for the n^{th} theoretical plate is as follows:

A vertical line from x_n to intersect the operating line at A_2 and the equilibrium curve at A_1 is drawn. From Equation (4), A_2 is expressed by $[(y_{n-1} + y_n)/2, x_n]$ and A_1 by (y_n, x_n) from Equation (6). Then the point A_3 which gives the vapor composition y_{n-1} of $(n-1)^{th}$ plate is determined by $\overline{A_1A_2} = \overline{A_2A_3}$. A horizontal line is drawn through A_3 to cut the operating line at A_5 $(y_{n-1}, x_{n,1})$ because the operating line (Figure 4) is similar in form to the ordinary operating line $y_{n-1} =$

$(L/V)x_{n,1} + (D/V)x_D$ and equilibrium curve at A_4 (y_{n-1}, x_{n-1}). Similarly, this operation is continued from x_D to the liquid composition equal to or less than x_W.

For convenience, in Figure 4 the broken line has been drawn symmetrically in y-direction with the equilibrium curve from the operating lines to show $\overline{A_1A_2} = \overline{A_2A_3}$, etc.

Minimum Number of Theoretical Plates

With the assumption that the liquid on a plate is mixed so well that the liquid composition is uniform at any point of the plate, the minimum number of theoretical plates at total reflux has been expressed by Fenske (7) as

$$S_m = \frac{\log (x_{i,D}/x_{j,D})(x_{j,W}/x_{i,W})}{\log \alpha_{ij}} \qquad (7)$$

On the contrary, as it has been assumed here that the liquid flows as a unidirectional plug flow on the plate, the following relation between the compositions of the top and bottom products can be derived

$$\frac{x_{i,D}}{x_{j,D}} = \alpha_{ij}^{2(N+1)}\left(\frac{x_{i,W}}{x_{j,W}}\right) \qquad (8)$$

where

$$\alpha_{ij}^{2(N+1)} = \left\{\left(\frac{K_{i,(D,N)}}{K_{j,(D,N)}}\right)\left(\frac{K_{i,N}}{K_{j,N}}\right)\right\} \times \ldots \times \left\{\left(\frac{K_{i,(n,n-1)}}{K_{j,(n,n-1)}}\right)\left(\frac{K_{i,(n-1)}}{K_{j,(n-1)}}\right)\right\} \times \ldots \times \left\{\left(\frac{K_{i,(1,W)}}{K_{j,(1,W)}}\right)\left(\frac{K_{i,W}}{K_{j,W}}\right)\right\} \qquad (9)$$

In Equation (9), $K_{i,(n,n-1)}$ is a mean value between $K_{i,n}$ and $K_{i,(n-1)}$. By rearranging Equation (8), the minimum number of theoretical plates is given approximately as

$$S_m = N_m + 1 \doteq \frac{\log\{(x_{i,D}/x_{j,D})(x_{j,W}/x_{i,W})\}}{2\log \alpha_{ij}} \qquad (10)$$

Thus, the minimum number of theoretical plates is nearly one half of that given by Fenske's equation (7). Under the assumptions just described.

Consideration of Liquid Mixing on Plate

In the present section, the component is being mixed by eddy diffusion as well as by the liquid flow on the plate. In such a case, Equation (4) is rewritten as

$$\frac{y_{n-1}+y_n}{2} = \left(\frac{L}{V}\right)\left\{x_n - \frac{D_eA\rho_L}{LM}\left.\frac{dx}{dz}\right|_{z=\frac{1}{2}Z}\right\} + \left(\frac{D}{V}\right)x_D = \left(\frac{L}{V}\right)\left[x_n - \frac{1}{N_{Pe}}\left.\frac{dx}{dw}\right|_{w=\frac{1}{2}}\right] + \left(\frac{D}{V}\right)x_D \qquad (11)$$

The liquid composition profile was given in our previous paper (*1*). That is, according to the mass balance on the plate, the basic equation for the eddy diffusion model has been derived as

$$\frac{D_eA\rho_L}{M}\left(\frac{d^2x}{dz^2}\right) - L\left(\frac{dx}{dz}\right) + (y_{n-1} - y_n)\frac{V}{Z} = 0 \qquad (12)$$

Equation (12) is rewritten into a dimensionless form

$$\frac{1}{N_{Pe}}\left(\frac{d^2x}{dw^2}\right) - \frac{dx}{dw} - \lambda E_{OG}(x - x^*_{n-1}) = 0 \qquad (13)$$

where x^*_{n-1} is the liquid composition in equilibrium with vapor from $(n-1)^{\text{th}}$ plate. With the boundary conditions

$$x = x_n \quad \text{at} \quad w = \frac{1}{2} \qquad (14)$$

$$\frac{dx}{dw} = 0 \quad \text{at} \quad w = 1 \qquad (15)$$

The solution of Equation (13) was

$$\frac{x - x^*_{n-1}}{x_n - x^*_{n-1}} = \frac{\exp\left\{(\eta + N_{Pe})\left(w - \frac{1}{2}\right)\right\}}{1 + \frac{\eta + N_{Pe}}{\eta}\exp\left(\eta + \frac{N_{Pe}}{2}\right)} + \frac{\exp\left(\frac{\eta + N_{Pe}}{2}\right)\exp\{-\eta(w-1)\}}{\exp\left(\eta + \frac{N_{Pe}}{2}\right) + \frac{\eta}{\eta + N_{Pe}}} \qquad (16)$$

where

$$\eta = \frac{N_{Pe}}{2}\left(\sqrt{1 + \frac{4\lambda E_{OG}}{N_{Pe}}} - 1\right) \qquad (17)$$

The composition gradient at the center of the plate is given with the derivative of Equation (16)

$$\left.\frac{dx}{dw}\right|_{w=\frac{1}{2}} = \frac{\eta(\eta + N_{Pe})\left\{1 - \exp\left(\eta + \frac{N_{Pe}}{2}\right)\right\}}{\eta + (\eta + N_{Pe})\exp\left(\eta + \frac{N_{Pe}}{2}\right)}(x_n - x^*_{n-1}) \qquad (18)$$

Substituting Equation (18) into Equation (11)

$$\frac{y_{n-1}+y_n}{2} = \left(\frac{L}{V}\right)[x_n + \{F(N_{Pe},\eta)\}(x_n - x^*_{n-1})] + \left(\frac{D}{V}\right)x_D \qquad (19)$$

where

$$F(N_{Pe},\eta) = \frac{\eta(\eta + N_{Pe})\left\{\exp\left(\eta + \frac{N_{Pe}}{2}\right) - 1\right\}}{N_{Pe}\left\{\eta + (\eta + N_{Pe})\exp\left(\eta + \frac{N_{Pe}}{2}\right)\right\}} \qquad (20)$$

Relationships of Equations (4), (6), and (19) are shown in Figure 5 on the x-y diagram for the case where the vapor composition from $(n-1)^{\text{th}}$ plate is y_{n-1}. In the case where the liquid flows as a plug flow and $F(N_{Pe}, \eta)$ is zero, the relation has been shown by the broken line for $N_{Pe} = \infty$, and the liquid composition at the center of n^{th} plate is given by A_2 as an abscissa of point B_7. When the liquid is completely mixed, the liquid composition x_n at the center of the plate coincides with the composition $x_{n,1}$ at the outlet, given by A_3 as an abscissa of point B_8 and shown by the dotted line for $N_{Pe} = 0$.

For any degree of liquid mixing on the n^{th} plate, the point B_3 lies somewhere between points B_7 and B_8 on the

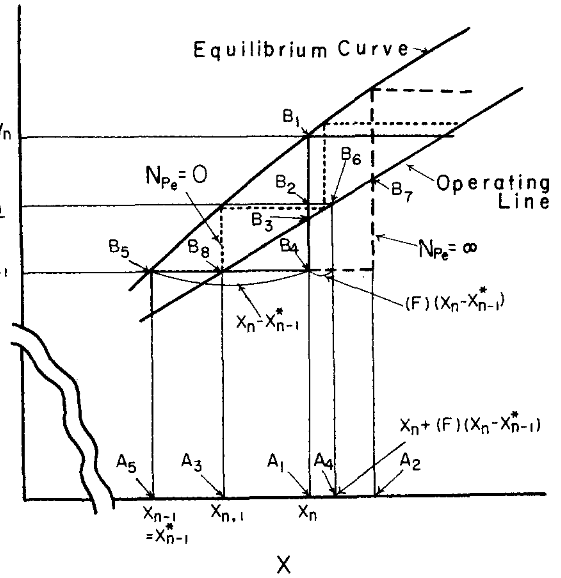

Fig. 5. Stepwise construction when mixing of liquid occurs on the plate. Dotted line for $N_{Pe} = 0$ represents the case of complete mixing, and broken line for $N_{Pe} = \infty$, the plug flow of liquid.

operating line. The vertical line from point B_3 cuts the equilibrium curve at B_1, which gives the composition of vapor leaving n^{th} plate. Point B_8 is obtained by the intersection of a horizontal line through $(y_{n-1} + y_n)/2$ with the operating line. The abscissa of B_8 is given by Equation (19) as $x_n + (F)(x_n - x^*_{n-1})$ by the point A_4. Here, x^*_{n-1} is the abscissa of B_5—the point on the equilibrium curve. As the degree of the mixing of liquid on the plate increases (i.e., N_{Pe} decreases), the value of F showing the distance $\overline{A_1A_4}$ increases, and point B_3 shifts from B_7 towards B_8. Thus, it is concluded that the number of theoretical plates depend upon the strength of the liquid mixing.

Number of Theoretical Plates for Any Degree of Mixing

In Figure 5, $\overline{B_1B_4}$ (on the vertical line extending from x_n), which is the liquid composition of the component under consideration, can be expressed as

$$\overline{B_1B_4} = y_n - y_{n-1} = m(x_n - x^*_{n-1}) \tag{21}$$

B_2 is the middle point of $\overline{B_1B_4}$, therefore

$$\overline{B_2B_3} = \frac{1}{2}(\overline{B_1B_4}) - \overline{B_3B_4} = \frac{m}{2}(x_n - x^*_{n-1}) - \overline{B_3B_4} \tag{22}$$

Also, in Figure 5, the slope of the operating line is

$$\frac{\overline{B_2B_3}}{(F)(x_n - x^*_{n-1})} = \frac{L}{V} \tag{23}$$

From Equations (22) and (23)

$$\overline{B_3B_4} = \left\{\frac{m}{2} - F\left(\frac{L}{V}\right)\right\}(x_n - x^*_{n-1}) \tag{24}$$

$\overline{B_1B_4}$, that is, $(y_n - y_{n-1})$, is divided into two parts by the operating line. The ratio of the parts is given by

$$\frac{\overline{B_3B_4}}{\overline{B_1B_3}} = \frac{\left\{\frac{m}{2} - (F)\left(\frac{L}{V}\right)\right\}(x_n - x^*_{n-1})}{\left\{\frac{m}{2} + (F)\left(\frac{L}{V}\right)\right\}(x_n - x^*_{n-1})} = \frac{\frac{\lambda}{2} - F}{\frac{\lambda}{2} + F} \tag{25}$$

Now a vertical line $\overline{B_1B_4}$ is drawn from B_1 (x_n, y_n) satisfying the ratio given by Equation (25). B_4 gives the vapor composition of $(n - 1)^{\text{th}}$ plate. A horizontal line is drawn through B_4 to cut the equilibrium curve at B_5 (x_{n-1}, y_{n-1}). This operation is continued to the desired composition of the products, and thus the number of theoretical plates is obtained.

For the complete mixing of the liquid, N_{Pe} and η are zero, and the limiting value of F expressed by Equation (20) becomes $\lambda E_{OG}/2$. Thus, when $E_{OG} = 1$ (for the theoretical plate), the ratio given by Equation (25) becomes zero. Then, the stepwise construction is shown with the dotted line for $N_{Pe} = 0$ in Figure 5.

Under the plug flow of the liquid, $F = 0$ for the limiting case of Equation (20), the ratio given by Equation (25) becomes 1, and the stepwise construction is shown with the broken line for $N_{Pe} = \infty$ in Figure 5.

However, in practice, it is difficult to know the liquid composition x_n at the center of the plate; therefore, the mean of the inlet and the outlet liquid compositions is used instead of x_n, as mentioned later. Thus the effect of mixing has been included in the plate efficiency.

The mean of the inlet and the outlet liquid compositions is represented by $x_n + (F)(x_n - x^*_{n-1})$, as shown in Figure 6, and the difference between this mean composition and the composition x_n at the center of the plate is given by $(F)(x_n - x^*_{n-1})$. The following relation between the efficiency $(E_{MV})_{1/2}$, based on the composition at the center of the plate, and the efficiency $(E_{MV})'_{1/2}$ for the mean of the inlet and the outlet compositions, has been derived from Figure 6 as follows:

$$\begin{aligned}\frac{(E_{MV})_{1/2}}{(E_{MV})'_{1/2}} &= \frac{(\overline{A_2A_3})/(\overline{A_1A_3})}{(A_5A_7)/(A_4A_7)} = \frac{\overline{A_4A_7}}{A_1A_3} = \frac{\overline{A_{10}A_7}}{A_{10}A_3} \\ &= \frac{\{x_n + (F)(x_n - x^*_{n-1})\} - x^*_{n-1}}{x_n - x^*_{n-1}} \\ &= 1 + F\end{aligned} \tag{26}$$

This relation is shown in Figure 7. For $\lambda E_{OG} < 1$, the difference between $(E_{MV})'_{1/2}$ and $(E_{MV})_{1/2}$ is 50% at the maximum for complete mixing, and the difference is smaller for the larger diameter of the column because the larger the diameter of the column, the larger the value

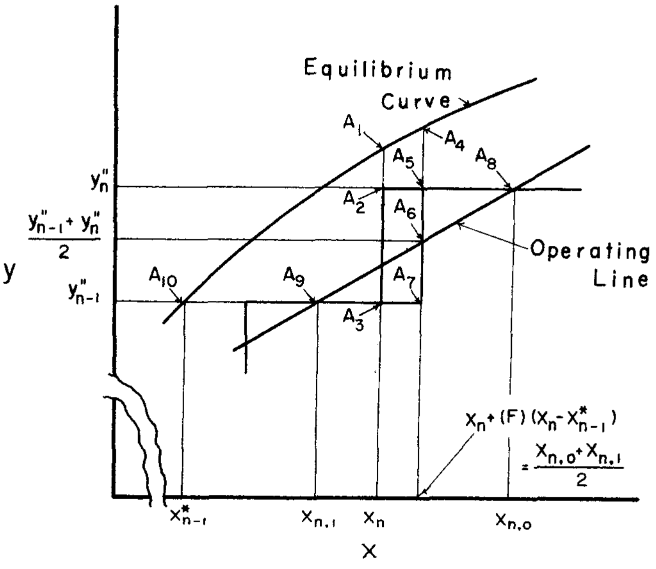

Fig. 6. Relation between the plate efficiencies $(E_{MV})_{1/2}$ and $(E_{MV})'_{1/2}$.

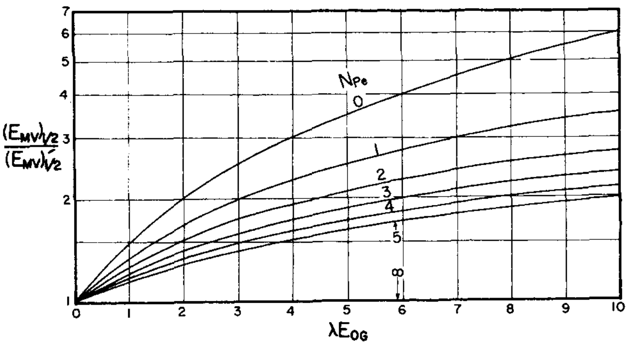

Fig. 7. Ratio of plate efficiencies $(E_{MV})_{1/2}$ and $(E_{MV})'_{1/2}$, given by Equation (26).

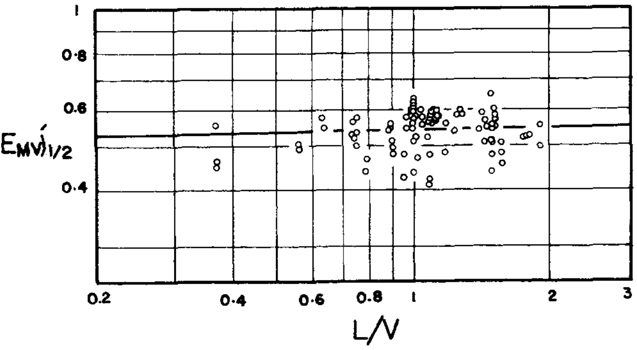

Fig. 8. Relation between modified plate efficiency $(E_{MV})'_{1/2}$ and L/V.

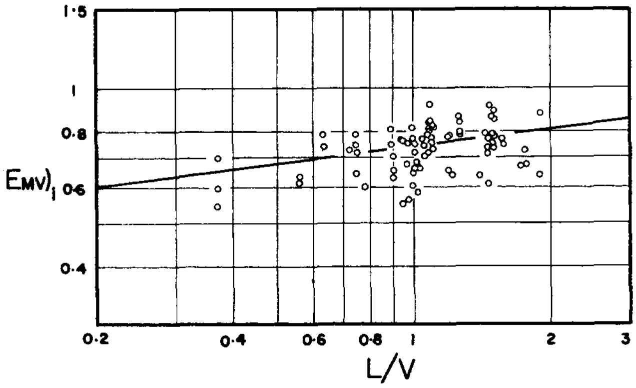

Fig. 9. Relation between Murphree's plate efficiency $(E_{MV})_1$ and L/V.

of N_{Pe}. Here, the plate efficiency $(E_{MV})'_{1/2}$ is for the plug flow of the liquid on the plate as an ideal case.

EMPIRICAL CORRELATION OF PLATE EFFICIENCIES $(E_{MV})'_{1/2}$

The variables affecting the plate efficiency can be divided into three main groups: system-property variables, operating variables, and tray-design variables. System-property variables depend upon the type and composition of the components. These are relative volatility, gas and liquid density, viscosity and diffusion coefficient, and surface tension. Operating variables include gas and liquid rates, temperature, and pressure. Tray-designs are tray dimensions: tray spacing, weir height, and design and arrangement of bubble caps.

A correlation including all the variables can only be reliable and is of extreme importance for the engineering purposes. Several attempts to correlate the plate efficiency with these variables have been made and various methods have been proposed to predict it. Out of these, the most commonly used method, originally proposed by Drickamer and Bradford (*8*) and subsequently modified and developed by O'Connell (*9*), is based upon an empirical relationship between Murphree's plate efficiency and the product of viscosity and relative volatility. This method, including only a few of the system property variables, gives satisfactory results only in the case of hydrocarbons distillation. Uhmoltz (*10*) and Jones (*11*) studied only the effect of tray-design variables and system variables, respectively. Chaiyavech et al. (*12*) attempted to evaluate and correlate the effect of only the system property variables with a perforated 1-in.-diam. plate. The applicability of the correlation to the industrial column is doubtful. The AIChE Research Commission's Distillation Research Program (*2*) studied the effects of nearly all the variables and proposed a method involving troublesome calculations. Besides this, it has a limited application to various other systems (*1*). More recently, English et al. (*13*) proposed an empirical correlation including most of the variables. This equation is not dimensionless and does not give satisfactory results as shown in Figure 12.

The modified Murphree's plate efficiency has been defined by Equation (1) with the vapor composition in equilibrium with the liquid at the center of the plate. However, it is practical to measure the composition of liquid at the outlet of the plate. Thus the mean of the compositions of the liquid at the inlet and the outlet of the plate is used instead of the liquid composition at the center of the plate. Thus the plate efficiency is written as

$$(E_{MV})'_{1/2} = \frac{y''_n - y''_{n-1}}{(y_n{}^*)' - y''_{n-1}} \tag{27}$$

where $(y_n{}^*)'$ is the vapor composition in equilibrium with the liquid composition x_n', which is the mean of the compositions of liquid at the inlet and the outlet of the plate. In the present study, an attempt has been made to correlate various variables with the efficiency defined above by Equations (27).

$(E_{MV})'_{1/2}$ calculated from the data reported by The University of Delaware (*2*) are plotted against L/V in

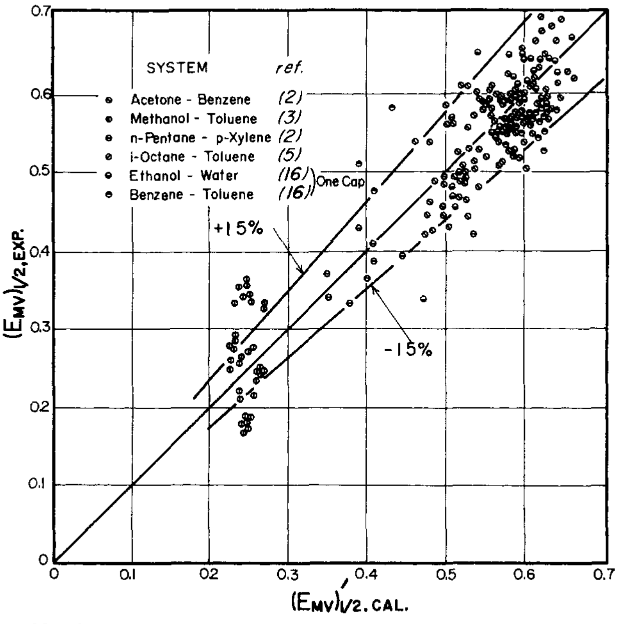

Fig. 10. Comparison of experimental values of plate efficiencies $(E_{MV})'_{1/2}$ and those calculated with Equation (28).

Figure 8. For the same data, Murphree's plate efficiencies $(E_{MV})_1$ are plotted against L/V in Figure 9. The value of $(E_{MV})_1$ increases with increase of L/V, but the value of $(E_{MV})'_{1/2}$ varies little with L/V. That is, the dependence of the plate efficiency $(E_{MV})'_{1/2}$ on the reflux ratio is much smaller than that of Murphree's plate efficiency $(E_{MV})_1$. The dependence of Murphree's plate efficiency $(E_{MV})_1$ on the reflux ratio increases with the increase of Peclet's number N_{Pe} as shown in Figure 2. On the other hand, the dependence of $(E_{MV})'_{1/2}$ on the reflux ratio decreases with the increase of N_{Pe} as shown in Figure 7. In other words, the larger the diameter of the distillation column, the greater the dependence of $(E_{MV})_1$ and the lesser the dependence of $(E_{MV})'_{1/2}$ on the reflux ratio.

Source of Data

Particular care has been taken in the selection of data. Accurately measured data are essential for the correlation study. Also, the effect of tray-design variables can be experienced only by a large-scale unit. The data of binary system reporting the compositions of the consecutive trays have been used. In the case where such data are not available, $(E_{MV})'_{1/2}$ has been calculated by the graphical method.

AIChE Research Commission's Final Reports (*2*), (*3*), and (*4*) include quite reliable and useful data for large-scale columns for various systems. Manning (*5*) reported plate efficiencies of a 5-ft.-diam. plate, using an *iso*octane and toluene system. The experimental values of physical properties used in the computation have been picked up from I.C.T., Perry's "Chemical Engineers' Handbook," and elsewhere. In the case of nonavailability, these values have been calculated with the methods recommended by Reid and Sherwood (*14*).

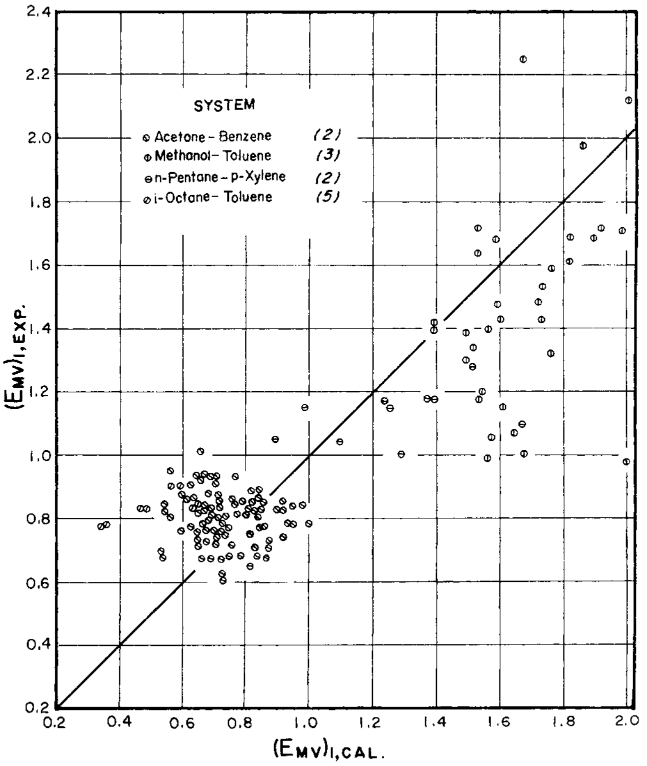

Fig. 11. Comparison of experimental values of Murphree's plate efficiencies $(E_{MV})_1$ and those calculated with Equation (28)': $(E_{MV})_1 = 0.1808\ (N_{ReV})^{0.448}\ (N_{ReL})^{-0.176} \times (N_{ScL})^{-0.374}\ (N_{Ca})^{-0.071}\ (\alpha)^{0.387}\ (Z \cdot h_w/Sa)^{-0.299}$.

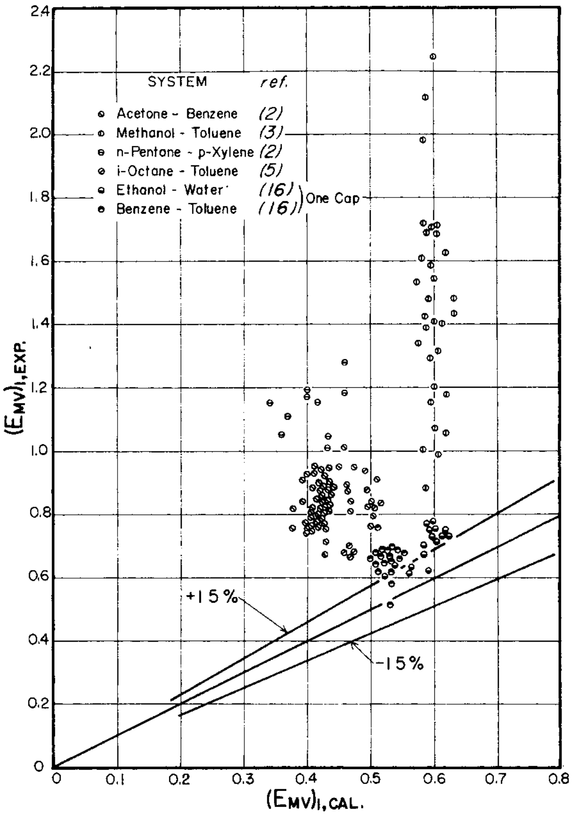

Fig. 12. Comparison of experimental values of Murphree's plate efficiencies $(E_{MV})_1$ and those calculated with English's correlation (13).

Correlation

The effects of important variables on plate efficiency have already been studied (*2-4, 8-13*). Keeping these in mind, the dimensionless groups involving the important physical property variables, design variables, and operating variables have been selected. They are, namely, Schmidt's liquid number $(\mu_L/\rho_L D_L)$; capillary number $(\mu_V u_V/\sigma)$; Reynold's liquid number $(4\Gamma/\mu_L)$; Reynold's vapor number $(d_{s1} u_V \rho_V/\mu_V)$; relative volatility α, and design group $(Z \cdot h_w/S_a)$. The groups have been calculated with the experimental or accurately calculated physical properties and dimensions of each plate. The physical properties have been determined with liquid composition x_n'.

The modified plate efficiencies $(E_{MV})'_{1/2}$ have been calculated with the reported data of various systems, i.e., acetone-benzene (*2*), *n*-pentane-*p*-xylene (*2*), methanol-toluene (*3*), *iso*octane-toluene (*5*), benzene-toluene (*16*), ethanol-water (*16*). The composition x_n' has been used for the calculation of efficiencies of each plate. The modified plate efficiencies have been correlated with the dimensionless groups by the least squares method using an NEAC2203 electronic computer.

The following correlation is obtained

$$(E_{MV})'_{1/2} = 0.1359 (N_{ReV})^{-0.192} (N_{ReL})^{0.242} (N_{ScL})^{0.095} \times (N_{Ca})^{0.085} (\alpha)^{-0.267} \left(\frac{Z \cdot h_w}{S_a} \right)^{0.076} \quad (28)$$

This correlation is strictly applicable to a single plate of the column using binary systems. Equation (28) expresses the experimental data of industrial scale columns quite satisfactorily with the standard deviation 0.0498.

By changing the constant only, this equation can be used also for laboratory scale columns having a plate with one cap. The value of the constant in this case has been calculated as 0.2699; the standard deviation, 0.0540.

Figure 10 shows the comparison of the calculated and the experimental values of the plate efficiencies. Similarly, Murphree's plate efficiency $(E_{MV})_1$ has been correlated as Equation (28)′ in Figure 11, with coefficient and exponents different from those in Equation (28). However, the standard deviation in this case is found to be 0.238.

The present correlation has been compared with a recently published correlation by English et al. (*13*). The efficiencies calculated with English's correlation for ordinary Murphree's plate efficiency $(E_{MV})_1$ are plotted in Figure 12. The experimental and calculated values show large variations in the case of industrial scale columns. So Equation (28) can be applied for the calculation of efficiencies of the rectifying columns with satisfactory reliability.

CONCLUSION

A method for the calculation of the number of theoretical plates, based on the composition x_n for the plug flow of liquid on the plate, has been developed, and it has been also extended to the case where mixing occurs. The minimum number of the theoretical plates for the plug flow is nearly one half of that for the complete mixing of the liquid.

Because it is difficult to determine the composition of the liquid at the center of the plate, the plate efficiencies $(E_{MV})'_{1/2}$ are calculated by Equation (27). The deviation between $(E_{MV})_{1/2}$ and $(E_{MV})'_{1/2}$ is shown by Equation (26) and Figure 7. $(E_{MV})'_{1/2}$ is little affected by the reflux ratio for large-scale columns. An empirical correlation is presented by Equation (28) for the calculation of the efficiency $(E_{MV})'_{1/2}$. It gives quite reliable results for the industrial columns.

II. Column Efficiencies

RELATION BETWEEN PLATES AND REFLUX RATIO

The number of plates required to rectify the mixture into the desired products depends upon the reflux ratio. Gilliland (*17*) correlated the number of theoretical steps S and the reflux ratio R as the functions of the minimum number of steps S_m and of the minimum reflux ratio R_m. This correlation is very complex and can be shown only on the graphs. Derived by means of McCabe and Thiele's methods (*6*), it implies the complete mixing of the liquid on the plate as described in Part I.[*] The modified plate efficiency gives most satisfactory results for practical columns; therefore, the composition gradient on the plate should not be neglected. Thus, for an ideal case, it can be assumed that the liquid on the plate is flowing as plug flow.

For various values of the relative volatility α, the number of theoretical plates is determined by the graphical method already described and the results are shown in Figure 13.[*] As the number of theoretical plates for the plug flow is nearly one-half that given in the case of a completely mixed liquid, the fractional number of theoretical plates is more important in the present case. The distillation capacity of each part of the plate is not the same due to the change of the liquid composition. Here, it is assumed that the differential part dN of a plate works to change the vapor composition by dy, and also dy is proportional to $y^* - y$

$$dy = k(y^* - y)dN \tag{29}$$

where k is a proportional constant, and y is the composition of the vapor on the fractional part of the plate.

Integrating Equation (29)

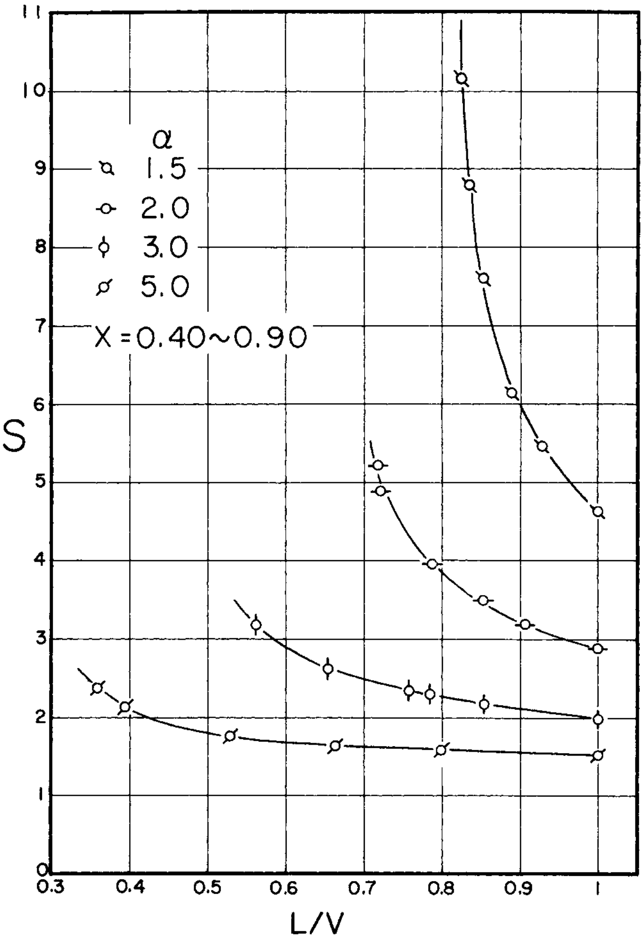

Fig. 13. Variation of number of steps for various values of relative volatility α.

---

[*] Part I contains Equations (1) through (28) and Figures 1 through 12.

$$N_f = \frac{1}{k}\int_{y_n}^{y} \frac{dy}{y^* - y} + C \qquad (30)$$

Now, at $y = y_n$, $N_f = 0$, and at $y = y_{n+1}$, $N_f = 1$

$$0 = \frac{1}{k}\int_{y_n}^{y_n} \frac{dy}{y^* - y} + C \qquad (31)$$

$$1 = \frac{1}{k}\int_{y_n}^{y_{n+1}} \frac{dy}{y^* - y} + C \qquad (32)$$

Therefore

$$C = 0 \qquad (33)$$

$$k = \int_{y_n}^{y_{n+1}} \frac{dy}{y^* - y} \qquad (34)$$

Equations (33) and (34) are substituted into Equation (30)

$$N_f = \frac{\displaystyle\int_{y_n}^{y} \frac{dy}{y^* - y}}{\displaystyle\int_{y_n}^{y_{n+1}} \frac{dy}{y^* - y}} = \frac{(N_{OY})_{y_n}^{y}}{(N_{OY})_{y_n}^{y_{n+1}}} \qquad (35)$$

Thus, the fractional number of plate has been calculated by the ratio of the transfer unit of the fractional part of the plate and the transfer unit of the complete plate.

In the same way as Gilliland's diagram, $(S - S_m)/(S + 1)$ are plotted against $(R - R_m)/(R + 1)$ in Figure 14. These points are not on a single curve, and the different curves result from different values of α. However, if $(S - 1)/(S_m - 1)$ is chosen instead of $(S - S_m)/(S + 1)$ as the ordinate, the correlation shown in Figure 15 is obtained. This correlation is expressed by a simple equation as

$$\frac{S - 1}{S_m - 1} = \left[\frac{R - R_m}{R + 1}\right]^{-1/3} \qquad (36)$$

The number of theoretical plates for a given reflux ratio can be easily determined by Equation (36).

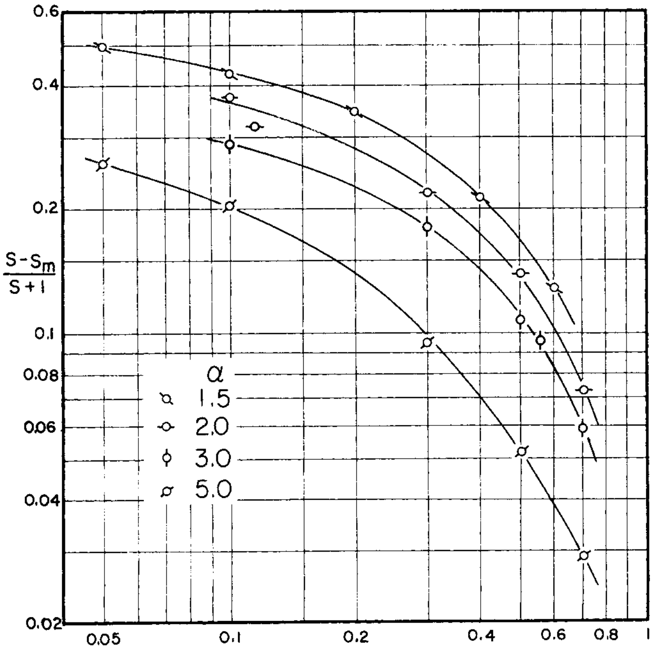

Fig. 14. Correlation between $(S - S_m)/(S_m + 1)$ and $(R - R_m) \div (R + 1)$ for various values of α.

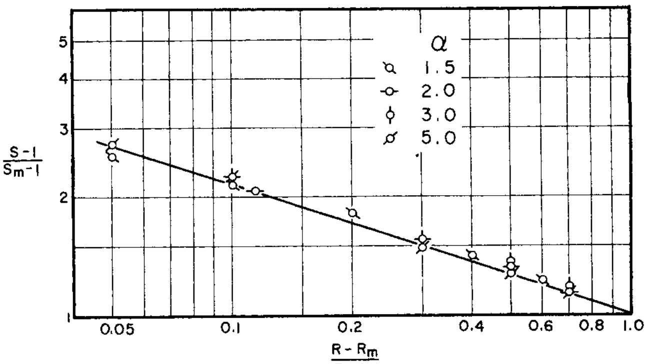

Fig. 15. Correlation between $(S - 1)/(S_m - 1)$ and $(R - R_m) \div (R + 1)$ for various values of α.

COLUMN EFFICIENCIES

The column efficiency, which is the ratio of the number of theoretical plates to that of practical plates, is of great importance for determination of the number of practical plates. However, there is no exact method for calculation of the column efficiency. For the case where the equilibrium curve can be represented by a straight line, the relation between the column efficiency and the Murphree's plate efficiency $(E_{MV})_1$ was given by Lewis (*18*).

With the same assumptions as Lewis (i.e., the equilibrium curve is a straight line and the plate efficiency is constant over the column), a relation between column efficiency E_T and modified plate efficiency $(E_{MV})_{1/2}$ defined by Equation (1) has been derived.

The equilibrium curve being a straight line is given by

$$y_n = mx_n + b_1 = \left(\frac{L}{V}\right)\lambda x_n + b_1 \qquad (37)$$

And the operating line is expressed by

$$y = \left(\frac{L}{V}\right)x_n + \left(\frac{D}{V}\right)x_D \qquad (38)$$

From Equation (4) and Equation (38), $(y_{n-1} + y_n)/2 = y$. Therefore, the line drawn symmetrically in y-direction with the equilibrium curve from the operating line is given as

$$y_{n-1} = \left(\frac{L}{V}\right)(2 - \lambda)x_n + \left\{2\left(\frac{L}{V}\right)x_D - b_1\right\} \qquad (39)$$

Thus, the number of theoretical plates is determined by the stepwise construction between the lines expressed by Equations (37) and (39) as shown in Figure 16.

Under the assumption that the plate efficiency is constant over the column, the number of practical plates is determined by the stepwise construction between the lines (40) and (41) as shown in Figure 16. If these two lines are expressed by

$$y_{n'} = a_2 x_{n'} + b_2 \qquad (40)$$

$$y_{(n-1)'} = a_3 x_{n'} + b_3 \qquad (41)$$

then the following relations are derived from the symmetry of the lines (40) and (41) from the line (38) in y-direction

$$a_2 + a_3 = 2\left(\frac{L}{V}\right) \qquad (42)$$

$$b_2 + b_3 = 2\left(\frac{D}{V}\right)x_D \qquad (43)$$

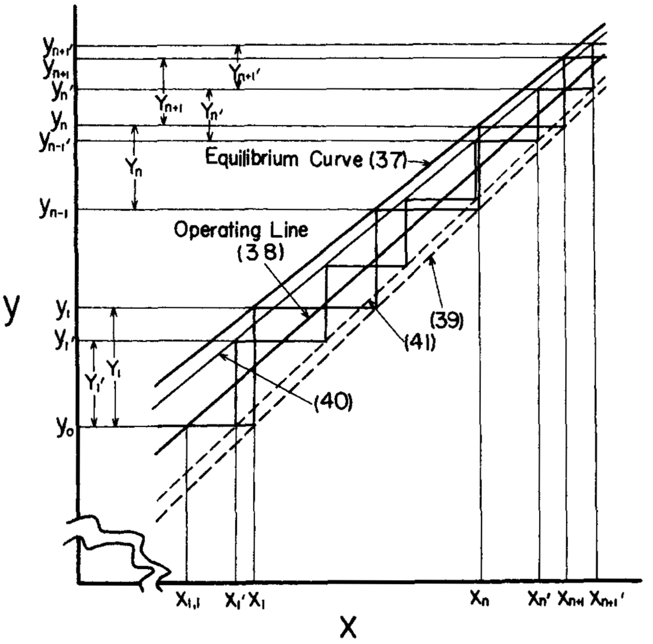

Fig. 16. Stepwise construction for the case when the equilibrium curve is a straight line. Steps drawn between lines (37) and (39) are for ideal plates, and those drawn between lines (40) and (41) are for a constant plate efficiency over the column.

Also, for the constant plate efficiency

$$(E_{MV})_{1/2} = \frac{a_2 - a_3}{m - a_3} = \frac{b_2 - b_3}{b_1 - b_3} \tag{44}$$

From Equations (42), (43), and (44)

$$a_2 = \left(\frac{L}{V}\right)\left\{\frac{2 - 2(E_{MV})_{1/2} + (E_{MV})_{1/2}\lambda}{2 - (E_{MV})_{1/2}}\right\} \tag{45}$$

$$a_3 = \left(\frac{L}{V}\right)\left\{\frac{2 - (E_{MV})_{1/2}\lambda}{2 - (E_{MV})_{1/2}}\right\} \tag{46}$$

$$b_2 = \frac{2\left(\frac{D}{V}\right)x_D - 2(E_{MV})_{1/2}\left(\frac{D}{V}\right)x_D + (E_{MV})_{1/2}b_1}{2 - (E_{MV})_{1/2}} \tag{47}$$

$$b_3 = \frac{2\left(\frac{D}{V}\right)x_D - (E_{MV})_{1/2}b_1}{2 - (E_{MV})_{1/2}} \tag{48}$$

At $x = x_n$, Y_n shown in Figure 16 is obtained by deducting Equation (39) from Equation (37)

$$Y_n = y_n - y_{n-1}$$

$$= 2\left(\frac{L}{V}\right)(\lambda - 1)x_n + 2\left\{b_1 - \left(\frac{D}{V}\right)x_D\right\} \tag{49}$$

Also the slope of line (39) can be written as

$$\frac{Y_n}{x_{n+1} - x_n} = \left(\frac{L}{V}\right)(2 - \lambda) \tag{50}$$

With Equations (49) and (50), a relation between Y_{n+1} and Y_n is obtained

$$Y_{n+1} = 2\left(\frac{L}{V}\right)(\lambda - 1)x_{n+1}$$

$$+ 2\left\{b_1 - \left(\frac{D}{V}\right)x_D\right\} = \frac{\lambda}{2 - \lambda}Y_n \tag{51}$$

Thus, the series $\{Y_1, Y_2, \ldots\ldots, Y_N\}$ is a geometrical progression and the summation of the series is

$$(\mathrm{SUM})_N = \sum_1^N Y_n = \frac{Y_1(1 - r^N)}{1 - r}$$

$$= \frac{Y_1(2 - \lambda)(1 - r^N)}{2(1 - \lambda)} \tag{52}$$

where

$$r = \frac{\lambda}{2 - \lambda} \tag{53}$$

In the same way, the relation between $Y_{(n+1)'}$ and $Y_{n'}$ is derived as

$$Y_{(n+1)'} = \left\{\frac{(E_{MV})_{1/2}\lambda - 2(E_{MV})_{1/2} + 2}{2 - (E_{MV})_{1/2}\lambda}\right\}Y_{n'} \tag{54}$$

And the summation of the series $\{Y_{1'}, Y_{2'}, \ldots\ldots, Y_{n'}, \ldots\ldots, Y_{N'}\}$ is given by

$$(\mathrm{SUM})_{N'} = \sum_1^{N'} Y_{n'} = \frac{Y_{1'}\{2 - (E_{MV})_{1/2}\lambda\}}{(E_{MV})_{1/2}(1 - \lambda)}(1 - r'^{N'}) \tag{55}$$

where

$$r' = \frac{(E_{MV})_{1/2}\lambda - 2(E_{MV})_{1/2} + 2}{2 - (E_{MV})_{1/2}\lambda} \tag{56}$$

Equating $(\mathrm{SUM})_N$ and $(\mathrm{SUM})_{N'}$

$$\frac{Y_1(2 - \lambda)}{2(1 - \lambda)}(1 - r^N) = \frac{Y_{1'}\{2 - (E_{MV})_{1/2}\lambda\}}{2(E_{MV})_{1/2}(1 - \lambda)}(1 - r'^{N'}) \tag{57}$$

The ratio of Y_1 and $Y_{1'}$ taken as shown in Figure 16, is

$$\frac{Y_1}{Y_{1'}} = \frac{x_1 - x_{1,1}}{x_{1'} - x_{1,1}}$$

$$= \frac{\frac{V}{L(2 - \lambda)}\left\{y_0 - 2\left(\frac{D}{V}\right)x_D + b_1\right\} - \left(\frac{V}{L}\right)\left\{y_0 - \left(\frac{D}{V}\right)x_D\right\}}{\frac{V\{2 - (E_{MV})_{1/2}\}}{L\{2 - (E_{MV})_{1/2}\lambda\}}\left\{y_0 - \frac{2\left(\frac{D}{V}\right)x_D - (E_{MV})_{1/2}b_1}{2 - (E_{MV})_{1/2}}\right\} - \left(\frac{V}{L}\right)\left\{y_0 - \left(\frac{D}{V}\right)x_D\right\}}$$

$$= \frac{2 - (E_{MV})_{1/2}\lambda}{(E_{MV})_{1/2}(2 - \lambda)} \tag{58}$$

From Equations (57) and (58)

$$r^N = r'^{N'} \tag{59}$$

Thus, the column efficiency E_T which is the ratio of the theoretical plate N and the practical plate N' is given by

$$\frac{1}{E_T} = \frac{N'}{N} = \frac{\log r}{\log r'}$$

$$= \frac{\log \dfrac{\lambda}{2-\lambda}}{\log \dfrac{(E_{MV})_{1/2}\lambda - 2(E_{MV})_{1/2} + 2}{2 - (E_{MV})_{1/2}\lambda}} \tag{60}$$

For various values of $(E_{MV})_{1/2}$, the relation between $1/E_T$ and λ is shown in Figure 17 with the solid lines. All the curves pass through a minimum at $\lambda = 1$, and it can also be confirmed theoretically by differentiating Equation (60) with λ. In Figure 17, broken lines represent Lewis' relation (*18*) for $(E_{MV})_1$. These curves do not show any minimum and their values decrease with increase of λ.

As the equilibrium curve is usually not a straight line, the value of λ varies with the composition. Therefore, Equation (60) cannot be used directly, and the mean value of λ should be used.

For the case when $\alpha = 5$ and $L/V = 1$ (as the most severe case), the number of theoretical plates and the number of practical plates for various values of $(E_{MV})_{1/2}$ are determined by the graphical method described in Part I. An example of this method is shown in Figure 18 for the case of $(E_{MV})_{1/2} = 0.8$. The number of theoretical plates N, determined with the stepwise construction between the solid curves, is 1.80 where the fractional number is calculated by Equation (35). Also, the number of practical plates N' is 2.95, which is obtained by the stepwise construction between the broken curves drawn with the ratio $(\overline{A_2A_3})/(\overline{A_1A_3}) = 0.8$. With these values, $1/E_T$ which is the ratio of N to N' has been calculated to be 1.64 (i.e., 2.95/1.80). In the same way, for various values of $(E_{MV})_{1/2}$, $1/E_T$ is determined for the case when the composition of the product at the top of the column is 0.95 and at the bottom is 0.05 (solid circles in Figure 19). Similarly, the blank circles in Figure 19 are those for the composition $x = 0.95$ at the top and 0.30 at the bottom.

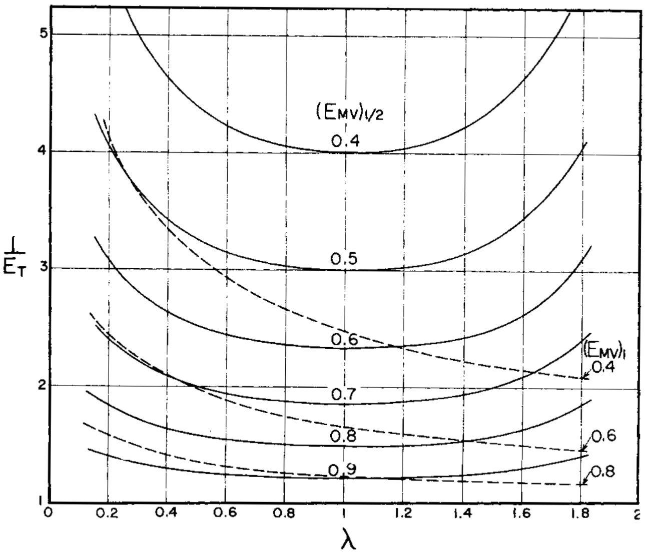

Fig. 17. Relation between $1/E_T$ and λ with $(E_{MV})_{1/2}$ as parameter. Broken lines show Lewis's relation (18).

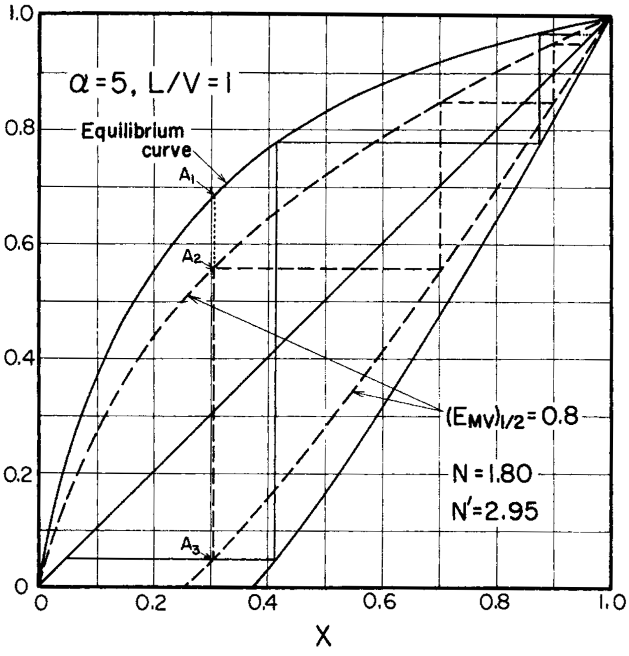

Fig. 18. Stepwise construction to determine the number of theoretical plates (solid curves) and the number of practical plates for $(E_{MV})_{1/2} = 0.8$ (broken curves).

Also, $1/E_T$ is calculated by Equation (60) for each case described above. For the case of $x = 0.95$ (top) and 0.30 (bottom), the value of λ is less than 1 for whole of the range of x, and the mean value of λ (i.e., $\overline{\lambda} = 0.473$) is used. The values calculated by Equation (60) with the mean value of λ is shown by the line (*a*) in Figure 19 and agrees well with those represented by the white circles.

In the case $x = 0.95$ (top) and 0.05 (bottom), λ varies from 0.214 to 3.40. As shown in Figure 17, $1/E_T$ shows a minimum at $\lambda = 1$. Therefore, for the calculation of $1/E_T$, it is necessary to divide the range of x into two regions: the first region I for $x = 0.05 \sim 0.30$ where $\lambda \geqq 1$, and the second region II for $x = 0.30 \sim 0.95$ where $\lambda < 1$. The average values of λ (i.e., $\overline{\lambda} = 1.894$) for the region I and $\overline{\lambda} = 0.473$ for the region II have been used.

As an example, when the plate efficiency $(E_{MV})_{1/2}$ is 0.8, the calculated values of $1/E_T$ are 2.10 and 1.60 for region I and region II, respectively. The numbers of theoretical plates N which are determined by the graphical method (see Part I) are 0.365 and 1.434 for the range $x = 0.05 \sim 0.30$ in region I and $x = 0.30 \sim 0.95$ in region II. Therefore, the number of practical plates N' for each region are 0.765 and 2.289, which are given by the product of $1/E_T$ and N. For whole of the region, the number of theoretical plates is 1.80 (i.e., 0.365 + 1.434) and the number of practical plates is 3.054 (i.e., 0.765 + 2.289). Thus, $1/E_T$, which is the ratio of these values, is 1.698 (i.e., 3.054/1.80). In the same way, $1/E_T$ is calculated by Equation (60) for various values of the plate efficiency $(E_{MV})_{1/2}$ and is shown by the solid line (*b*) in Figure 19. The agreement between the line (*b*) and the solid circles is good. Therefore, by dividing the composition range of x into several regions (if necessary) and with the mean value of λ in each region, it is possible to estimate quite accurately the column efficiency E_T by using Equation (60) for a given value of the plate efficiency $(E_{MV})_{1/2}$.

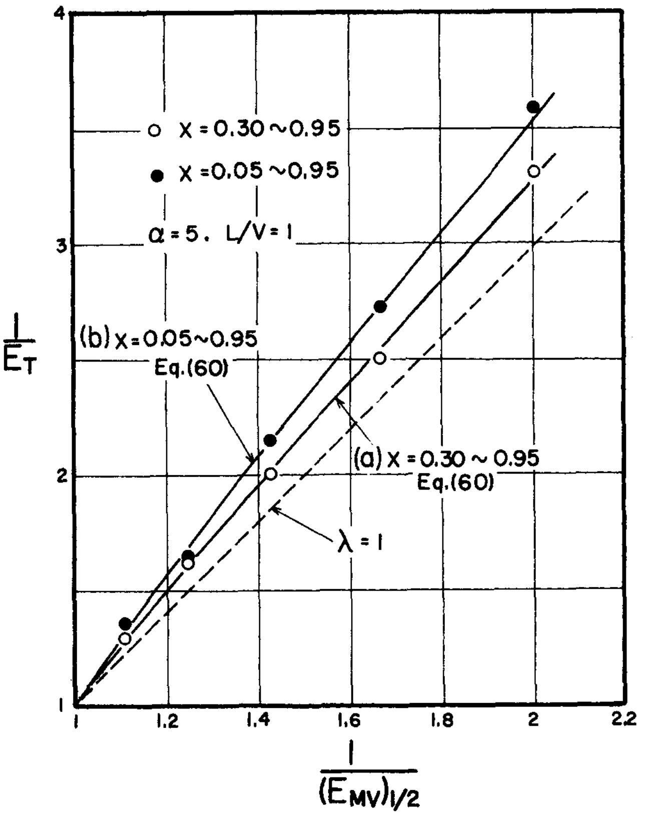

Fig. 19. Comparison of column efficiencies E_T calculated by Equation (60) and those obtained by the graphical method described in Figure 18. Broken line represents the values of $1/E_T$ calculated by Equation (60) at $\lambda = 1$, where $1/E_T$ becomes minimum.

CONCLUSION

A simple relation between the number of theoretical plates and the reflux ratio is obtained in Equation (36) as a function of the minimum number of stages and the minimum reflux ratio.

A relation between the column efficiency E_T and the modified plate efficiency $(E_{MV})_{1/2}$ is derived and given by Equation (60). It is explained that this equation can also be used to estimate E_T, when the equilibrium curve is not a straight line, by dividing the calculation into several parts for $\lambda \geqq 1$ and $\lambda < 1$.

NOTATION

A = cross-sectional flow area of the liquid segment on the plate, sq.cm.

D = flow rate of top product, mole/sec.

D_e = eddy diffusivity, sq.cm./sec.

D_L = diffusivity of liquid, sq.cm./sec.

d_{s1} = equivalent diameter of slot, cm.

$(E_{MV})_1$ = Murphree's plate efficiency based on vapor in equilibrium with the liquid leaving the plate

$(E_{MV})_0$ = Murphree's plate efficiency based on vapor in equilibrium with the liquid entering the plate

$(E_{MV})_{1/2}$ = modified plate efficiency based on vapor in equilibrium with the liquid at the center of the plate

$(E_{MV})'_{1/2}$ = modified plate efficiency based on vapor in equilibrium with the mean of the liquid compositions at the inlet and the outlet of the plate

E_{OG} = overall point efficiency

E_T = column efficiency

F = function of N_{Pe} and η, Equation (20)

h_w = weir height, cm.

K = equilibrium ratio

L = liquid flow rate in the enriching section, mole/sec.

L' = liquid flow rate in the exhausting section, mole/sec.

M = molecular weight

m = slope of equilibrium curve

N = number of theoretical plates

N' = number of practical plates

N_{Ca} = capillary number, $\mu_V u_V/\sigma$

N_f = fractional number of plate

N_{OY} = transfer unit

N_{Pe} = Peclet's number, $Z^2/D_e t_L$

N_{ReL} = liquid Reynold's number, $4\Gamma/\mu_L$

N_{ReV} = vapor Reynold's number, $u_V d_{s1} \rho_V/\mu_V$

N_{ScL} = liquid Schmidt's number, $\mu_L/\rho_L D_L$

R = reflux ratio

r = ratio of geometrical series in Equation (52) and presented by Equation (53)

r' = ratio of geometrical series in Equation (55) and presented by Equation (56)

S = number of steps

S_a = sum of area of all slots on one plate, sq.cm.

t_L = contacting time of liquid with vapor, sec.

u_V = vapor velocity at slot, cm./sec.

V = vapor flow rate in the enriching section, mole/sec.

V' = vapor flow rate in the exhausting section, mole/sec.

w = z/Z

W = flow rate of bottom product, mole/sec.

x = mole fraction of more volatile component in liquid

x_n = liquid composition at the center of n^{th} plate

x_n' = $(x_{n,0} + x_{n,1})/2$

x^*_{n-1} = liquid composition in equilibrium with vapor of $(n-1)^{th}$ plate

y = mole fraction of more volatile component in vapor

Y_n = $y_n - y_{n-1}$

y_n'' = practical vapor composition from n^{th} plate

y_n^* = vapor composition in equilibrium with x_n

(y_n^*) = vapor composition in equilibrium with x_n'

z = distance from inlet weir, cm.

Z = distance from inlet weir to outlet weir, cm.

α = relative volatility

Γ = liquid flow rate per mean unit width of the plate, g./cm. · sec.

η = presented by Equation (17)

λ = $m(V/L)$

μ = viscosity, g./cm. · sec.

ρ = density, g./cc.

σ = surface tension, dyne/cm.

Suffix

D = top product

i, n = i component on n^{th} plate

j, n = j component on n^{th} plate

L = liquid

m = minimum

n = number of the n^{th} theoretical plate in the enriching section

n' = number of the n'^{th} practical plate

n^0 = number of the n^{0th} theoretical plate in the exhausting section

$n, 0$ = inlet of n^{th} plate where $w = 0$

$n, 1$ = outlet of n^{th} plate where $w = 1$

V = vapor

W = bottom product

LITERATURE CITED

1. Onda, K., and O. Kobayashi, *Kagaku Kogaku*, **28**, 828 (1964).
2. AIChE (Am. Inst. Chem. Engrs.) Res. Comm., "Tray Efficiencies in Distillation Columns," *Final Rept., Univ. Delaware* (1958).
3. AIChE (Am. Inst. Chem. Engrs.) Res. Comm., "Tray Efficiencies in Distillation Columns," *Final Rept., State College N. Carolina* (1959).
4. AIChE (Am. Inst. Chem. Engrs.) Res. Comm., "Tray Efficiencies in Distillation Columns," *Final Rept., Univ. Mich.* (1960).
5. Manning, E., Jr., S. Marple, and G. P. Hinds, Jr., *Ind. Eng. Chem.*, **49**, 2051 (1957).
6. McCabe, W. L., and E. W. Thiele, *Ind. Eng. Chem.*, **17**, 605 (1925).
7. Fenske, M. R., *Ind. Eng. Chem.*, **24**, 482 (1932).
8. Drickamer, H. G., and J. R. Bradford, *Trans. Am. Inst. Chem. Engrs.*, **39**, 319 (1943).
9. O'Connell, H. E., *Trans. Am. Inst. Chem. Engrs.*, **42**, 741 (1946).
10. Umholtz, C. L., and M. Van Winkle, *Ind. Eng. Chem.*, **49**, 226 (1957).
11. Jones, P. D., and M. Van Winkle, *Ind. Eng. Chem.*, **49**, 232 (1957).
12. Chaiyavech, P., and M. Van Winkle, *Ind. Eng. Chem.*, **53**, 187 (1961).
13. English, G. E., and M. Van Winkle, *Chem. Eng.*, **70**, 241 (1963).
14. Reid, R. C., and T. K. Sherwood, "The Properties of 'Gas & Liquid' Their Estimation and Correlation," McGraw-Hill, New York (1966).
15. Coulson, J. M., and J. F. Richardson, "Chemical Engineering," Vol. 2, p. 404, Pergamon Press, London (1955).
16. Rhodes, F. H., and P. G. Slachman, *Ind. Eng. Chem.*, **29**, 51 (1937).
17. Gilliland, E. R., *Ind. Eng. Chem.*, **32**, 1220 (1940).
18. Lewis, W. K., *Ind. Eng. Chem.*, **28**, 399 (1936).

Manuscript received April 22, 1970; revision received August 31, 1970; paper accepted September 5, 1970.

Phase Equilibrium of Carbon Dioxide in the Methane-Carbon Dioxide-*n*-Decane System

AMOS YUDOVICH, R. L. ROBINSON, JR., and K. C. CHAO

School of Chemical Engineering
Oklahoma State University, Stillwater, Oklahoma 74074

Carbon dioxide occurs in varying concentrations in natural gases and crude oils. A knowledge of the phase behavior of carbon dioxide in hydrocarbon systems has applications in petroleum production and refining operations. The methane-carbon dioxide-decane system studied in this work represents a simplified model of natural systems in which carbon dioxide appears in combination with light gases and heavy hydrocarbons.

A chromatographic technique was used in the present study to determine vaporization equilibrium ratios of carbon dioxide at infinite dilution in methane-decane solutions. Since carbon dioxide is often present at low concentrations in natural systems, the state of infinite dilution is not an unrealistic one. Of more importance is the fact that these data yield useful information on interactions of carbon dioxide with methane and decane that, when analyzed in terms of a suitable model, permits predictions of the behavior of carbon dioxide at finite concentrations.

The present authors recently completed a study of the partial volumetric behavior of carbon dioxide at infinite dilution in gaseous methane. Results of that study have been combined with the present data to determine the nonideality of carbon dioxide in carbon dioxide-methane-decane liquid mixtures. Such information rarely has been available for ternary liquid mixtures at elevated pressures. The activity coefficients thus obtained are correlated based on a combined Scatchard-Hildebrand and Flory-Huggins model.

VAPOR LIQUID EQUILIBRIUM BY GAS-LIQUID CHROMATOGRAPHY

Many investigators have obtained equilibrium data at essentially infinite dilution using the gas-liquid chromatographic (GLC) technique (*1* to *8*), including high-pressure systems (*9* to *11*). Equilibrium properties of solutions determined from GLC elution data by previous investigators agreed with those obtained from static methods. A comprehensive review of the nonanalytical uses of chromatograph has been presented by Kobayashi, Chappelear, and Deans (*12*).

Martin and Synge (*13*) and others (*5*, *14*) derived the basic relations between vapor-liquid equilibrium at infinite dilution and GLC parameters. One such expression is

$$K_i = \frac{\left(\frac{\rho_L}{\rho_G}\right) V_L}{V_{R_i} - V_G} \tag{1}$$

If the carrier gas is soluble in the stationary liquid and its mole fraction in the liquid phase at equilibrium is x_1, the total moles of the stationary phase, that is, including the dissolved carrier gas, will be

---

Correspondence concerning this article should be addressed to Prof. K. C. Chao, School of Chemical Engineering, Purdue University, Lafayette, Indiana 47907. Amos Yudovich is with Union Carbide Corp., Chicago, Illinois 60638.